

fractions were 90.59 ± 1.36 , 30.31 ± 0.87 , 31.70 ± 0.40 , 55.40 ± 0.12 , 52.96 ± 0.53 , 20.90 ± 0.46 , 23.34 ± 0.25 and 6.27 ± 0.38 .

As observed in Figure 3, near competitive inhibition was exerted by the purified extract (EAE^P) on commercially available α -amylase. The K_m for α -amylase control was 1.81 mM, whereas in the presence of inhibitor, an increase was observed (2.22 mM). As evident in case of competitive inhibitions, the V_{max} values were constant (0.011 mM/min) even after the introduction of inhibitor into the reaction mixture. Likewise, Rey *et al.*¹³ studied the mode of antidiabetic activity by crude extracts of *P. peruviana* fruit. Their results revealed that it was able to inhibit maltase in a competitive manner. The K_m (1.110) in control, changed to 7.087 on addition of the crude extract, whereas V_{max} remained constant (0.009 mM/min). However, no such kinetic study is available pertaining to α -amylase inhibitory activity of endophytic actinobacteria of *M. koenigii*.

The antidiabetic activity is believed to be due to the presence of measurable amount of phenolics, which summed up to 32.36 ± 3.31 and 2.21 ± 1.57 mg/g of the extract in terms of the catechol and gallic acid equivalents. The presence of phenol moieties has previously been associated with the inhibition of carbohydrate hydrolysing enzymes¹⁴.

This study suggested that endophytic actinobacteria from *M. koenigii* possess significant antidiabetic potential which might help in preventing or slowing down the progress of the disease. It is important to consider that Acarbose, the commercial drug used to treat type 2 diabetes mellitus is also produced industrially by the actinomycete, i.e. *Actinoplanes* sp.¹⁵. Further study on the ethyl acetate extract may help develop chemical entities for clinical use.

1. Midhet, F. M., Al-Mohaimeed, A. A. and Sharaf, F. K., *Saudi Med. J.*, 2010, **31**, 768–774.
2. Sinha, T. and Bandopadhyay, A., *Int. J. Res. Pharm. Sci.*, 2012, **3**, 360–368.
3. Saini, S. C. and Reddy, G. B. S., *Am. J. Phyomed. Clin. Ther.*, 2015, **3**, 363–368.
4. Kesari, N., Gupta, R. K. and Watal, G., *J. Ethnopharmacol.*, 2004, **97**, 247–251.
5. Tembhurne, S. V. and Sakarkar, D. M., *J. Med. Plant Res.*, 2010, **4**, 2418–2423.
6. Vinuthan, M. K., Girish, K. V., Ravindra, J. P., Jayaprakash and Narayana, K., *Indian J. Physiol. Pharmacol.*, 2004, **48**, 348–352.
7. Saini, P., Gangwar, M. and Kaur, A., *Int. J. Biol. Chem. Sci.*, 2015, **2**, 180–188.
8. Garvie, E. I., In *Bergey's Manual of Systematic Bacteriology* (ed. Sneath, P. H. A.), Williams and Wilkins, 1986, pp. 1071–1075.
9. Kazeem, M. I., Adamson, J. O. and Ogunwande, I. A., *BioMed. Res. Int.*, 2013; doi:10.1155/2013/527570.
10. Mehni, A. M. and Shahdadi, F., *Int. J. Biosci.*, 2014, **4**, 224–228.
11. Lehninger, A. L., Nelson, D. L. and Cox, M. M., *Lehninger Principles of Biochemistry*, W. H. Freeman & Co, 2008, 5th edn.
12. Tanaka, M., *J. Int. Med. Res.*, 2012, **40**, 1295–1303.
13. Rey, D. P., Ospina, L. F. and Aragón, D. M., *Rev. Colomb. Cienc. Quím. Farm.*, 2015, **44**, 72–89.
14. Meng, S., Cao, J., Fen, Q., Peng, J. and Hu, Y., *J. Evid-Based Complementary Altern. Med.*, 2013; doi:10.1155/2013/801457.
15. Li, K. T., Zhou, J., Wei, S. J. and Cheng, X., *Bioresour. Technol.*, 2012, **118**, 580–583.

ACKNOWLEDGEMENT. We thank the Punjab Agricultural University (PAU), Ludhiana for financial and technical support.

Received 23 June 2016; revised accepted 1 April 2018

P. SAINI*
M. GANGWAR

Department of Microbiology,
College of Basic Sciences,
Punjab Agricultural University,
Ludhiana 141 004, India

*For correspondence.
e-mail: saini.preeti7777@gmail.com

Reactivation of minor scars to major landslides – a satellite-based analysis of Kotropi landslide (13 August 2017) in Himachal Pradesh, India

On 13 August 2017, a massive landslide occurred close to the village of Kotropi (near Kotropi bus stop) in Mandi district, Himachal Pradesh, India. It occurred on National Highway 154, the road between Mandi and Pathankot. Media reports suggest that a section of the slope totally collapsed and two buses of the Himachal State Transport Corporation along with few other vehicles were buried under the debris. News reports also suggest that there have been 46 fatalities from the incident. Around 300 m of the highway has been completely buried under debris, thus disrupting communication on an important route¹.

Rugged topography, deformed rock formations and steep slopes make the Himalayas a highly landslide-prone mountain belt. The landslides in this region are recorded to be triggered by rainfall and earthquakes^{2,3}. With both the triggering parameters, it is seen that the pre-existing condition of the slope has an important control on the occurrence of new landslides. Scars of pre-existing minor landslides make a particular slope more vulnerable to a major landslide event.

Satellite images are useful for rapid damage and morphological assessment of landslides in the Himalaya^{4,5}. Post-event

Resourcesat-2 LISS-IV Mx and Cartosat-2S data were acquired by ISRO on 15 and 16 August 2017 over the landslide-affected area through emergency payload programming. Analysis of Cartosat-2S image shows the occurrence of a large landslide in the area near Kotropi bus stop (Figure 1). The landslide zone is a near a thrusted contact (Main Central Thrust) between Shali group (dolomite and brick red shale) in the north and Siwalik group (sandstone and shale) in the south. The landslide is a ‘debris-flow’ type with a rotational failure mechanism⁶. It has long runout zone, which clearly suggests that heavy rainfall

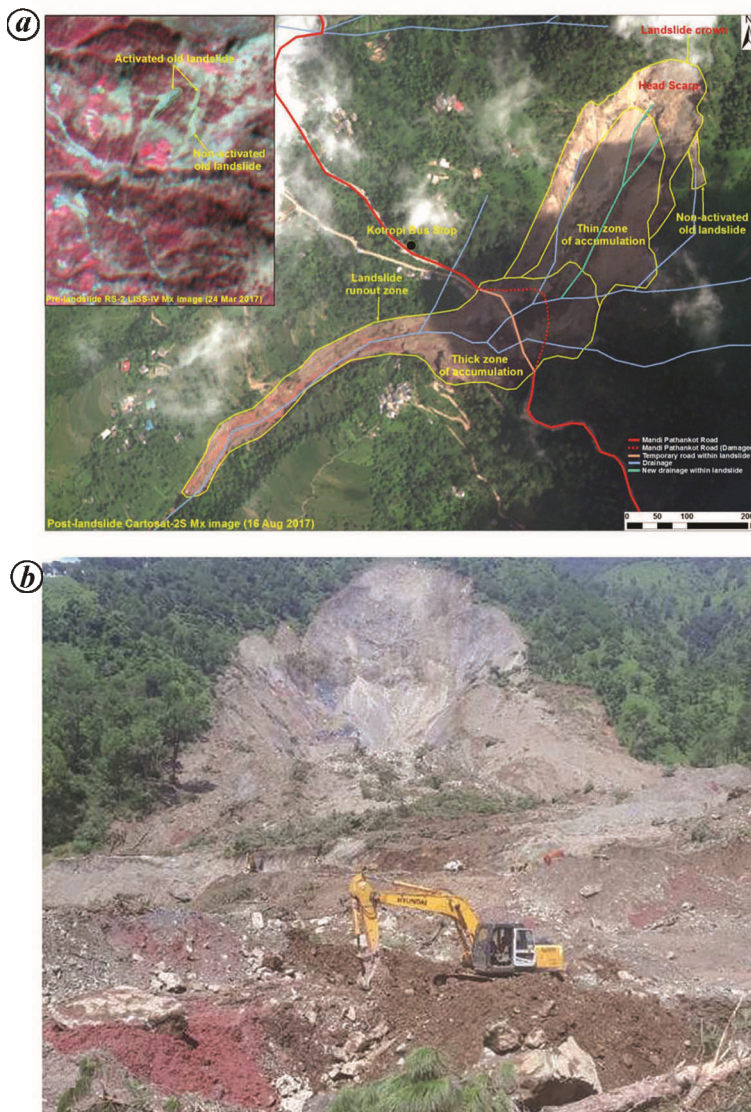


Figure 1. *a*, Assessment of Kotropi landslide using Cartosat 2S image. (Inset) Pre-landslide Resourcesat-2 LISS-IV Mx image. *b*, Field photograph of the landslide from news media (source:www.jagran.com).

is the main triggering factor. The area of the landslide is 133,674 m² and width is 190 m, while the runout length is 1155 m. Pre-landslide Resourcesat-2 LISS-IV Mx data (24 March 2017) of the area shows the presence of two existing landslide scars on the slope face (inset Figure 1 *a*). This indicates that the slope was prone to a major failure.

The occurrence of this landslide exemplifies that pre-existing scars on steep slope faces are potential areas for large future landslides. These scars not only indicate the instability of the slope material, but also expose bare soil from where rainwater seeps in. This increases pore pressure of the soil, eventually leading to a complete slope failure.

Considering the situation of Kotropi landslide, we examined ISRO's image archives to further investigate, if such small scars have resulted in mega landslides (Table 1). Three distinct examples from the recent past were identified, from which it is clear that previous minor landslide scars have indicated an eventual total slope failure. These landslides are: (a) Salna landslide (July 2007) in Chamoli district, Uttarakhand, India. (b) Sunkoshi landslide (August 2014) in the Sunkoshi river, Nepal. (c) Mantam landslide (August 2016) in Sikkim, India.

The Salna landslide was triggered by heavy rainfall during July 2007. The general topography of the region is steep,

with slopes ranging from 18° to 63°. The elevation of the crown and tip of the landslide is 1636 and 1261 m respectively. The Salna landslide is a translational rock slide, i.e. the failure had taken place along a planar surface of rupture. Its length (crown to tip) is 530 m, with a maximum width of 260 m at the centre of the landslide⁷. Analysis of the pre-event Cartosat-1 image of the slope face clearly shows that the slope bears some previous landslide scars (Figure 2 *a*). From the image, five distinct, minor landslides are seen on the slope face. The occurrence of these scar clusters indicates an unstable slope. Further, there are no other scars in the adjoining slopes, which reiterates the observation that this particular

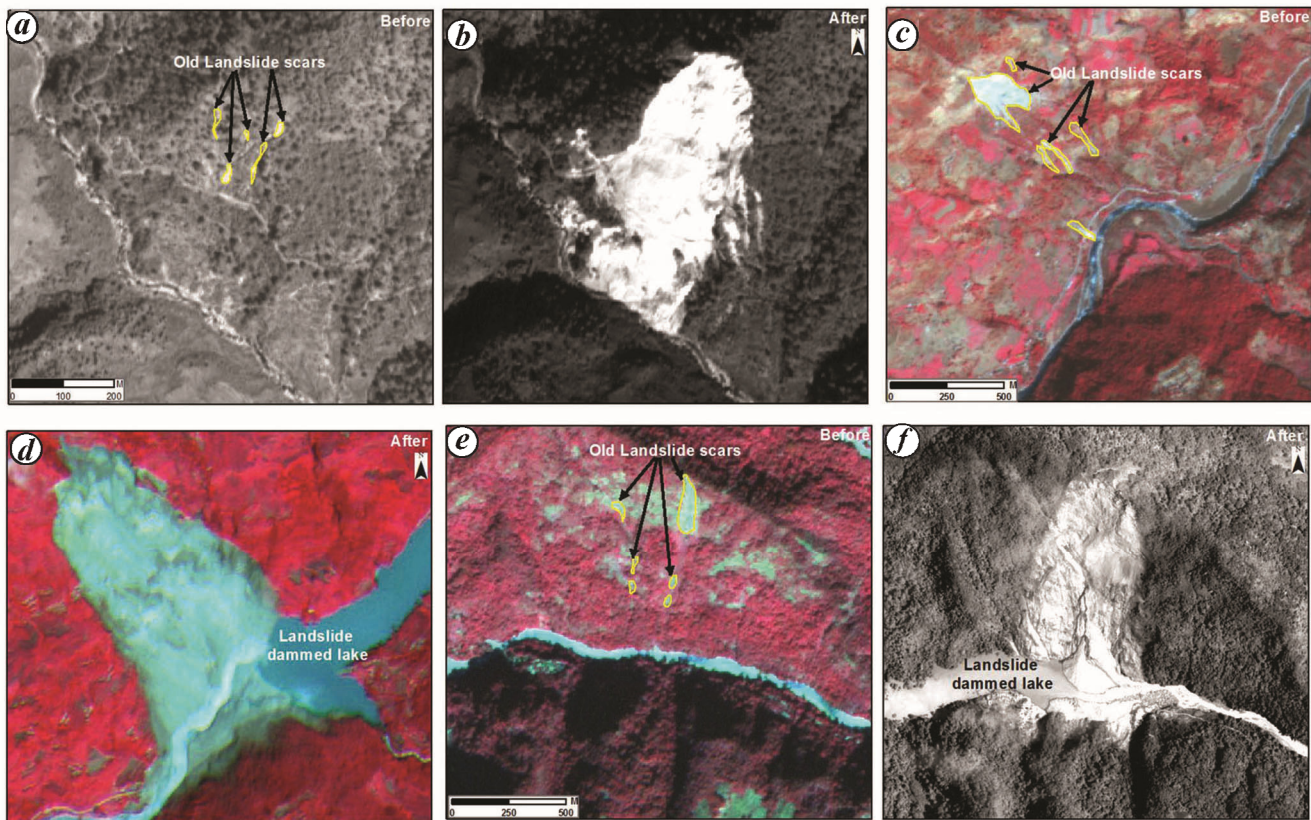


Figure 2. *a*, Pre-event Cartosat-1 image showing scars on slope. *b*, Post-event Cartosat-1 image showing Salna landslide. *c*, Pre-event LISS-IV Mx image showing crown and small landslides. *d*, Post-event LISS IV image of Sunkoshi landslide. *e*, Pre-event LISS-IV Mx image showing small landslide on ridge line. *f*, Post-event Cartosat-1 image of Mantam landslide.

Table 1. Satellite images used in the study

Landslide	Satellite	Acquisition	Sensor resolution (m)
Salna	Cartosat-1 (pre-event)	6 April 2006	2.5
	Cartosat-1 (post-event)	16 December 2007	2.5
Sunkoshi	Resourcesat-2 LISS-IV Mx (pre-event data)	27 February 2013	5.8
	Resourcesat-2 LISS-IV Mx (post-event data)	5 August 2014	5.8
Mantam	Resourcesat-2 LISS-IV Mx (pre-event data)	9 November 2013	5.8
	Cartosat-2 (post-event data)	15 August 2016	1
Kotropi	Resourcesat-2 LISS-IV Mx (pre-event data)	24 March 2017	5.8
	Resourcesat-2 LISS-IV Mx (post-event data)	15 August 2017	5.8
	Cartosat-2S Mx (post-event data)	16 August 2017	1.6

zone of the slope was unstable. These landslide scars eventually culminated into a large landslide after receiving heavy rainfall (Figure 2 *b*). The landslide completely buried the road with material displaced from the crown. The Nagol Gad river was pushed 25 m to its right bank by the landslide. Fortunately, no damming of the river occurred due to the landslide⁷.

The Sunkoshi landslide in Nepal was also triggered by heavy rainfall. It

occurred on 2 August 2014 near Jure village (close to Mankha) located in the Sunkoshi river valley in the central region of Nepal. The length of the landslide was ~1.3 km and maximum width around 650 m (ref. 5). The slope of the affected area was between 40° and 45°, with two small intermittent scarp sections. Over time, multiple small landslides have initiated from these two scarp sections. In the pre-event Resourcesat-2 LISS-IV Mx image, it is seen that a considerably large

and permanent head scarp has formed in the upslope area with small landslides originating from it. The three small scars are seen to have been formed in the upper scarp region (Figure 2 *c*). Another small landslide is seen at the bottom of the slope partly affecting the road. The large exposed head scarp and the small landslides clearly indicate that the section of the slope was completely under stress. Therefore, due to intense rainfall, the entire slope section failed resulting in

a massive landslide (Figure 2 *d*). The resultant landslide debris completely blocked the Sunkoshi river, forming a 2.2 km long impounded lake (Figure 2 *d*). A total of 19 houses built along the banks of the river were completely inundated by the landslide-impounded lake⁸.

Another large valley-blocking landslide occurred on 13 August 2016 near Mantam village in Sikkim due to heavy rainfall. The width of the landslide was 530 m in the middle and length 790 m (ref. 9). The pre-event Resoussesat-2 LISS-IV Mx image shows a landslide scar originating from the top of the ridge line (Figure 2 *e*). There are also a number of small landslides present, indicating that the slope face was under stress. These exposed landslide scars may have further aided in rainwater infiltration into the soil, thus building up pore pressure resulting in slope failure (Figure 2 *f*). The debris from the landslide blocked the flow of the Kanaka river/Tolung Chu, which is one of the main tributaries of the Teesta river. The water impoundment caused by the debris deposited on the river valley resulted in the formation of an artificial lake of 2.2 km length and 209 m width at the lake head⁹. Consequent rise in water level has led to submergence of the bridge over Kanaka river and washed away about 300 m stretch of road. Five houses in the Mantam village were also submerged.

Landslide scars are tell-tale signatures of stressed slope faces. Though isolated scars may not pose a serious threat for a potential large landslide, a cluster of scars on a single slope face may eventually lead to a complete slope failure. In the case of Kotropi landslide and the subsequent three examples cited here, a cluster of scars present on the slope face eventually led to the occurrence of large landslides in the presence of a triggering event. It is noteworthy that all these landslides are large in dimension (greater than 500 m in length) with the Sunkoshi and Mantam landslides resulting in the blocking of rivers, thus posing threat to downstream human settlements.

The Himalayan slopes, especially in Uttarakhand and Himachal Pradesh, are scarred by landslide occurrences, many of which may be clustered on the single slope faces and adjoining narrow river valleys. These scars are typically narrow and elongated in the downslope direction and adjacent to ridge lines. It is imperative to monitor such scars and adopt adequate slope stability measures in order to avoid the chances of an eventual large landslide damaging roads and buildings.

1. www.indiatoday.in
2. Martha, T. R. *et al.*, *Landslides*, 2015, **12**(1), 135–146.
3. Martha, T. R. *et al.*, *Landslides*, 2017, **14**(2), 697–704.
4. Martha, T. R. *et al.*, *Landslides*, 2017, **14**(1), 373–383.

5. Roy, P., Martha, T. R. and Vinod Kumar, K., *Curr. Sci.*, 2014, **107**(12), 1961–1964.
6. <https://employee.gsi.gov.in/cs/groups/public/documents/document/b3zp/mtyx/~edisp/dcp01gsigov161798.pdf>
7. Martha, T. R. *et al.*, *IEEE Geosci. Remote Sensing Lett.*, 2010, **7**(3), 582–586.
8. www.iciimod.org/?q=14356
9. Martha, T. R., Roy, P. and Vinod Kumar, K., *Curr. Sci.*, 2017, **113**(7), 1228–1229.

ACKNOWLEDGEMENTS. This note is an outcome of the disaster support work carried out under the Decision Support Centre activities of National Remote Sensing Centre (NRSC). We thank the Disaster Management Support (DMS) division and NRSC Data Centre (NDC) of NRSC for their timely support. We also thank the Deputy Director (Remote Sensing Application Area), Associate Director and Director (NRSC) for their support and guidance.

Received 22 August 2017; revised accepted 27 April 2018

PRIYOM ROY*
TAPAS R. MARTHA
NIRMALA JAIN
K. VINOD KUMAR

*Geosciences Group,
National Remote Sensing Centre,
Indian Space Research Organisation,
Hyderabad 500 037, India*

*For correspondence.
e-mail: roy.priyom@gmail.com